scientific reports

Check for updates

OPEN

Transcutaneous auricular vagus nerve stimulation inhibits food intake and body weight gain through the orexin dependent pathway in high fat diet mice

Yingying Zhang[1,2,3,4,7], Dake Song[4,7], Ruixia Liu[4], Hengxin Gong[4], Chuan Wang[1], Ming-gao Zhao[2]✉ & Kun Zhang[3,4,5,6]✉

Obesity represents a significant global health challenge, adversely affecting both physical and mental well-being. Neuromodulation techniques have demonstrated efficacy in promoting weight loss by regulating appetite. Recently, transcutaneous vagus nerve stimulation (taVNS) has garnered considerable attention. This study aims to investigate the effects of taVNS on food intake, body weight, and blood glucose levels in mice subjected to a high-fat diet (HFD), and to explore its potential mechanisms. Balb/c male mice were randomly assigned to three groups: control group, HFD + sham electroacupuncture group, and HFD + taVNS group ($n = 10$). The taVNS group received daily 30-min sessions of intermittent stimulation at 10 Hz and 1.0 mA in the bilateral cymba conchae for one week. Weight and dietary intake measurements were recorded daily at regular intervals, and fasting blood glucose levels were assessed for each group after one week of intervention. Additionally, the wet weight of adipose tissue in the epididymis, scapula, and groin was measured and recorded. Pathological changes in the liver were observed using Oil Red O and HE staining techniques. Various lipid indicators and orexin levels in mouse plasma were quantified via colorimetric and ELISA methods. To elucidate the mediating effects of brain regions on the action of taVNS, relevant neural circuits were mapped through C-fos expression, viral tracking, and chemogenetic methodologies. According to the research findings, taVNS can effectively reduce appetite and weight gain, enhance insulin sensitivity, and ultimately exert a hypoglycemic effect via the orexin-dependent neural circuit of the paraventricular nucleus-lateral hypothalamus. This suggests that taVNS is a promising treatment strategy for both obesity and diabetes.

Keywords Orexin-A, High-fat diet, Transcutaneous auricular vagus nerve stimulation, Slimming, Food intake

Abbreviations

HFD	High-fat diet
VNS	Vagus Nerve Stimulation
taVNS	Transcutaneous auricular vagus nerve stimulation
ABVN	Auricular branch of the vagus nerve
LH	Lateral hypothalamus

[1]Department of Pharmacology, School of Pharmacy, Shaanxi University of Chinese Medicine, Xianyang 712046, Shaanxi, China. [2]Precision Pharmacy and Drug Development Center, Department of Pharmacy, Tangdu Hospital, Fourth Military Medical University, Xinsi Road 1, Xi'an 710038, Shaanxi, China. [3]Key Laboratory of Acupuncture and Medicine of Shaanxi Province, Shaanxi University of Chinese Medicine, Xianyang 712046, Shaanxi, China. [4]Department of Pharmacology, School of Pharmacy, Fourth Military Medical University, Xi'an 710032, Shaanxi, China. [5]Research Institution, Xijing Hospital, Fourth Military Medical University, Xi'an 710032, Shaanxi, China. [6]Department of Pharmacy, Xijing Hospital, Fourth Military Medical University, Xi'an 71000, Shaanxi, China. [7]Yingying Zhang and Dake Song contributed equally to this work. ✉email: minggao@fmmu.edu.cn; kunzhang1900@163.com

PVN	Paraventricular nucleus
OXA	Orexin A
TC	Total cholesterol
TG	Triglycerides
LDL-C	Low-density lipoprotein cholesterol
HDL-C	High-density lipoprotein cholesterol
AAV	Adeno-associated viral vector
OxR	Orexin receptor
FG	Fluoro-Gold
PRV	Pseudomonas virus
DREADD	Designer receptor exclusively activated by designer drugs
WAT	White adipose tissue
FBG	Fasting blood glucose
GAD1	Glutamate decarboxylase 1

With the development of the economy and the continuous improvement of living standards, there is a growing trend that human eating habits are shifting towards high-fat and high-sugar diets. The surplus energy is stored in adipose tissue once energy intake exceeds individual energy expenditure, thereby leading to obesity[1]. A high fat diet (HFD) is considered as the major contributor to obesity development[2]. Furthermore, excessive energy intake can result in metabolic disorders, which may induce not only hyperglycemia and dyslipidemia but also metabolic diseases such as type 2 diabetes. Hence, multifaceted and effective prevention, together with treatment strategies become imperative for the rising prevalence of obesity. Currently, vagus nerve electrical stimulation (VNS) has been utilized in the treatment of various diseases, including epilepsy[3], refractory depression[4], traumatic brain injury[5], Parkinson's disease[6], and other conditions. Researches from neuroanatomy show that the only branch of the vagus nerve on the body surface is auricular branch of the vagus nerve (ABVN)[7], which mainly distributes within the external auditory meatus and concha (cymba conchae and cavum conchae), and the cymba conchae are supplied exclusively by the ABVN[8]. Thus, transcutaneous auricular VNS (taVNS) is a form of non-invasive VNS, as a promising electrical therapy. taVNS has been shown to regulate feeding and body weight in mice[9,10] yet its potential mechanism in the brain remains unknown.

The objective of this study is to evaluate the effect of taVNS on body weight and food intake in HFD mice. C-Fos staining in the whole brain was performed to identify the brain regions responsible for mediating taVNS' function. It can be concluded that taVNS inhibits the activity of LH (lateral hypothalamus) by activating the GABAergic projection from the PVN (paraventricular nucleus) area, which suppresses the orexin secretion by the LH. This research indicated that taVNS as an effective treatment for HFD induced obesity and uncovered the underlying mechanism.

Materials and methods

Experimental animals

Male Balb/C mice aged 5 to 7 weeks were obtained from the Experimental Animal Center of the Fourth Military Medical University in Xi'an, China. The mice were maintained and bred under standard laboratory conditions (12-h light/12-h dark cycle, temperature range of 22–26 ℃, and relative humidity of 55–60%) with access to water and chow ad libitum. In addition, they were randomly divided into three groups: a control group (CON), a HFD plus sham electrical acupuncture (SEA) group, and an HFD plus taVNS group, with 10 mice in each group. Except for the control group, the remaining two groups were fed with a HFD. The duration of the dietary intervention and tVNS lasted for 7 days. The number of animals used and their suffering were minimized to the greatest extent as possible. All experimental procedures adhered to the Guide for the Care and Use of Laboratory Animals (NIH), the Animal Research: Reporting of in vivo Experiments (ARRIVE) guidelines; and all of the experiments involving mice were conducted under protocols approved by the Animal Care and Use Committee of the Fourth Military Medical University (IACUC-20221227).

TaVNS and SEA

After being anesthetized with isoflurane, an EA therapy instrument (CMNS6-2, Wuxi Jiajian Medical equipment Co., LTD, China) was utilized for continuous intervention for 30 min daily over a span of 7 days, targeting the bilateral cymbae conchae of the mice. The stimulation parameters were applied as reported previously[11,12], at an intensity of 1.0 mA, a frequency of 10 Hz, and a train on-time of 2 s and off-time of 3 s. Electrodes were connected to the bilateral cymba conchae of the mice, and slight tremors in the outer auricles were observed as a positive response. The stimulation point for SEA was the earlobe, outside of the auricular branch of the vagus nerve innervated area.

Materials

HFD was purchased from Chongqing Tengxin Biotechnology Co., Ltd (H10060) (Chongqing, China). Normal diet was purchased from Jiangsu Medison biomedical Co., Ltd (MD17122) (Yangzhou, China). The composition and energy density of the two experimental diets are shown in the table below (Tables 1 and 2). In addition, the fat of HFD mainly comes from lard and soybean oil, while the fat of normal diet only comes from soybean oil. Isoflurane was sourced from Shenzhen Reward Life Technology Co., Ltd (Shenzhen, China). Blood glucose test strips and the related device were obtained from Sannuo Biosensing Co., Ltd (Changsha, China). Additionally, ELISA kit of insulin (Mouse INS, E-EL-M1382), total cholesterol (TC, E-BC-K109-M), triglyceride (TG, E-BC-K261-M), low-density lipoprotein cholesterol (LDL-C, E-BC-K205-M), high-density lipoprotein cholesterol (HDL-C, E-BC-K221-M), and Orexin A (OXA, E-EL-MO860) were obtained from Wuhan Eliruit Biotechnology

Component	Normal diet (kcal %)	High-fat diet (kcal %)
Protein (%)	22.47	20
Carbohydrate (%)	65.42	20
Fat (%)	12.11	60
total	100	100

Table 1. Composition of experimental diets.

Component	Normal diet (kcal /g)	High-fat diet (kcal /g)
Protein	0.8988	0.8
Carbohydrate	2.6168	0.8
Fat	1.0899	5.4
Total	4.6055	7

Table 2. Energy density of the experimental diet.

Co., Ltd (Wuhan, China). Almorexant hydrochloride was procured from Med ChemExpress (MCE), Catalog No.: HY-10,805 A (New Jersey, USA). The c-Fos (9F6) Rabbit mAb #2250 antibody was acquired from Cell Signaling Technology (Massachusetts, USA).

Weight and blood glucose testing

In this experiment, the food intake and body weight of the mice were measured at 8:00 a.m. After one week's intervention, the fasting blood glucose levels of the mice were assessed following a 16-h fasting period. Throughout this time, the mice had free access to the drinking water.

Fat pad and liver weight measurements

All mice were sacrificed by cervical dislocation. Parameters to be recorded included weights of the liver and the fat in the epididymis, scapula, inguinal area. Epididymal fat is situated between the tail of the epididymis and the distal testis end of the testis, while scapular fat is found beneath the scapula. Inguinal fat is located in the subcutaneous tissue of the groin, connecting the abdomen and thighs.

Oil red O staining

Liver tissue was fixed in 4% paraformaldehyde overnight and subsequently sliced into 10 μm thick sections using a freezing microtome. The sections were then immersed in isopropyl alcohol containing 0.5% Oil Red O for 15 min, followed by a brief rinse with 60% isopropyl alcohol. After washing with deionized water, the size and content of the lipid droplets were observed through an optical microscope.

Hematoxylin-eosin (HE) staining

Paraffin-embedded liver tissue was sectioned into 3 μm thick slices, which were then dewaxed with xylene and stained with hematoxylin for 3 to 5 min. Following this, the samples were dehydrated using a gradient of acidic ethanol solutions, clarified with 100% xylene, and stained with eosin for 5 min. After dehydration and clarification, the sections were sealed with neutral resin. The morphological changes of the liver were subsequently examined under a light microscope (Olympus VS200).

Total cholesterol, triglycerides, low-density lipoprotein cholesterol, and high-density lipoprotein cholesterol determination

A colorimetric method was employed to quantify the levels of total cholesterol (TC), triglycerides (TG), low-density lipoprotein cholesterol (LDL-C), and high-density lipoprotein cholesterol (HDL-C) in mouse plasma in conformity with the instructions of the reagent manufacturer. Besides, the ELISA method was used to assess the concentrations of insulin and orexin in mouse plasma.

Immunofluorescence staining

After removing the brains of mice and fixing them overnight in 4% paraformaldehyde, the brain was sectioned into 20 μm slices. The antibodies employed included rabbit anti-phospho-cfos (Ser32) at a dilution of 1:200 (Cell Signaling Technology, Inc.) and Alexa Fluor 488 goat anti-mouse IgG at a dilution of 1:1,000 (Invitrogen). Fluorescent images were captured with an Olympus Fluoview FV1000 confocal microscope.

Stereotactic injection

Adeno-associated viruses (AAVs) was packaged by Obio Biotechnology Co., Ltd. Shanghai, China., Fluoro-Golds (FG) was purchased from Fluorochrome (Colorado, USA), pseudorabies virus (PRV) purchased from BrainVTA (Cat.No.: P03001, Wuhan, China). Mice were anesthetized with 1% sodium pentobarbital, and a brain stereotaxic instrument was employed for the precise locating of LH area (A/P(-)1.22 mm, M/L(±)1.0 mm, D/V(-)5.15 mm) or PVN area (A/P(-)0.94 mm, M/L(±)0.25 mm, D/V(-) 4.8 mm). Four weeks postsurgery,

both hM4Di, hM3Dq and mCherry mice received an injection of the DREADD (Designer receptor exclusively activated by designer drugs) agonist (CAS: 2250025-92-2, i.p.) at a dosage of 0.5 mg/kg. Brains were collected 5 days post-FG (50 nl) or 7 days post-PRV (1 μl) injection.

Data analysis

All data were examined using GraphPad Prism version 8.0.1, with the results presented as the means ± SD. Unpaired Student's t-test was conducted for difference comparisons between the two groups. One-way ANOVA was utilized to analyze data from more than two groups, followed by the Tukey post hoc test. $P < 0.05$ was considered statistically significant.

Results

TaVNS reduced food intake and body weight in HFD mice

The experimental schematic of this part is shown in Fig. 1a. In comparison to mice with standard diet, HFD mice exhibited increased food intake and body weight. These indexes were significantly attenuated by taVNS (Fig. 1b, $F_{(2, 27)} = 8.543$, $p = 0.0013$; Fig. 1c, $F_{(2, 27)} = 13.89$, $p < 0.0001$; Fig. 1d, $F_{(2,15)} = 35.98$, $p < 0.0001$; Fig. 1e, $F_{(2,15)} = 133.5$, $p < 0.0001$). Furthermore, the elevated fasting blood glucose (FBG) levels in the HFD mice were also ameliorated by taVNS (Fig. 1f, $F_{(2, 27)} = 70.63$, $p < 0.0001$). White adipose tissue (WAT) serves as an energy reservoir during periods of high caloric intake[13], contributing to obesity[14]. Consequently, we dissected the epididymal and inguinal adipose tissues. These results demonstrated that the fat pad wet weight in the HFD mice were significantly higher than those in the CON group. In contrast to the HFD group, the weight of fat in taVNS-treated mice were significantly reduced (Fig. 1g, $F_{(2, 27)} = 10.32$, $p = 0.0005$; Fig. 1h, $F_{(2, 27)} = 13.55$, $p < 0.0001$; Fig. 1i, $F_{(2, 27)} = 7.018$, $p = 0.0035$). Compared to the HFD mice, the levels of TG, LDL-C, and TC in the plasma were decreased following taVNS intervention (Fig. 2a, $F_{(2, 27)} = 8.797$, $p = 0.0011$; Fig. 2b, $F_{(2, 27)} = 8.241$, $p = 0.0016$; Fig. 2c, $F_{(2, 27)} = 36.37$, $p < 0.0001$), whereas the level of HDL-C was elevated (Fig. 2d, $F_{(2, 27)} = 25.13$, $p < 0.0001$). Moreover, taVNS also led to a reduction in insulin levels in HFD mice (Fig. 2e, $F_{(2, 27)} = 9.019$, $p = 0.001$). And the weight of the liver were also significantly diminished (Fig. 2. f, Fig. 2g, $F_{(2, 27)} = 14.40$, $p < 0.0001$). In addition, there was no significant difference between CON group and HFD + taVNS group. In summary, these results suggest that taVNS may be an effective treatment for mitigating obesity induced by a HFD.

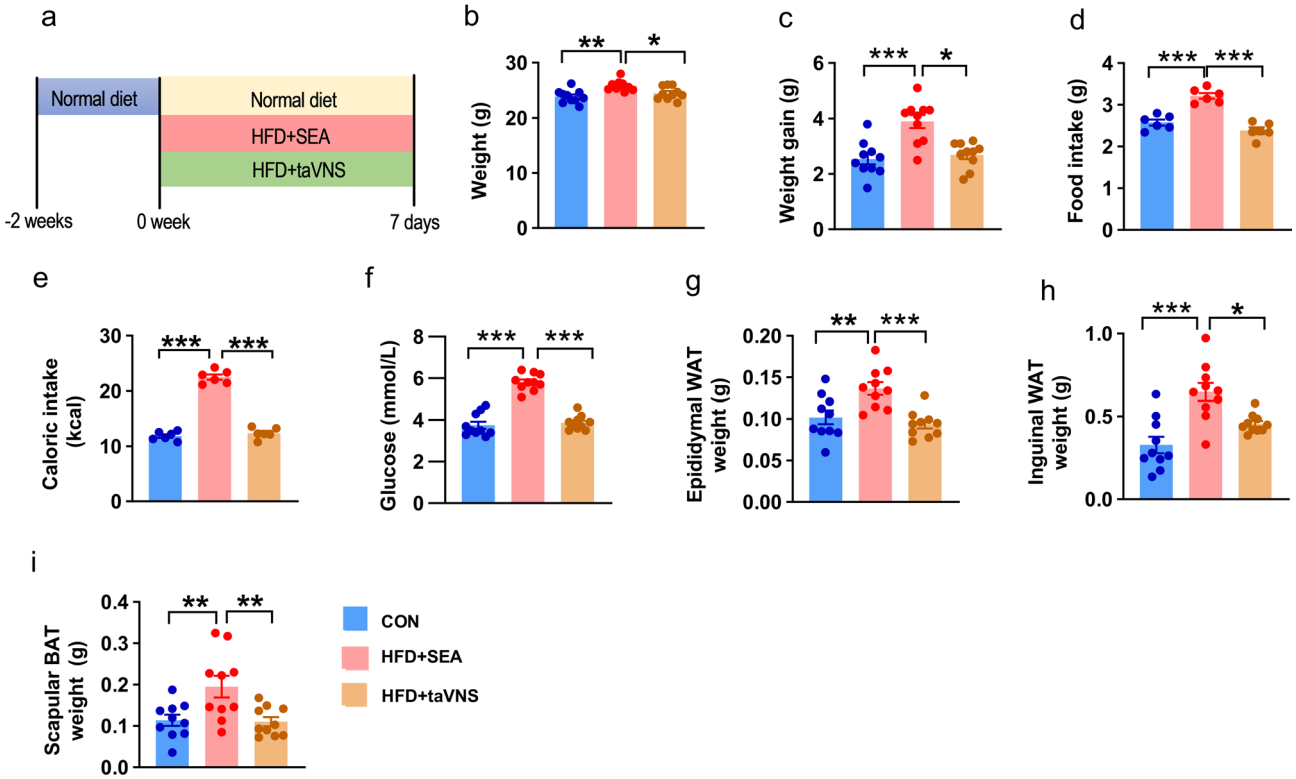

Fig. 1. taVNS significantly reduces food intake, body and fat pad weight in HFD mice. (**a**) Schematic of the experimental procedure. (**b**, **c**) Changes in body weight and body weight of mice after 7 days of taVNS intervention. (**d**, **e**) Food intake and calories intake of mice. (**f**) FBG levels of mice in each group. (**g**–**i**) Fat pad wet weight in the epididymis, groin, and scapula regions. $n = 10$ in each group. Statistical significance was denoted as $^{*}P < 0.05$, $^{**}P < 0.01$, $^{***}P < 0.001$.

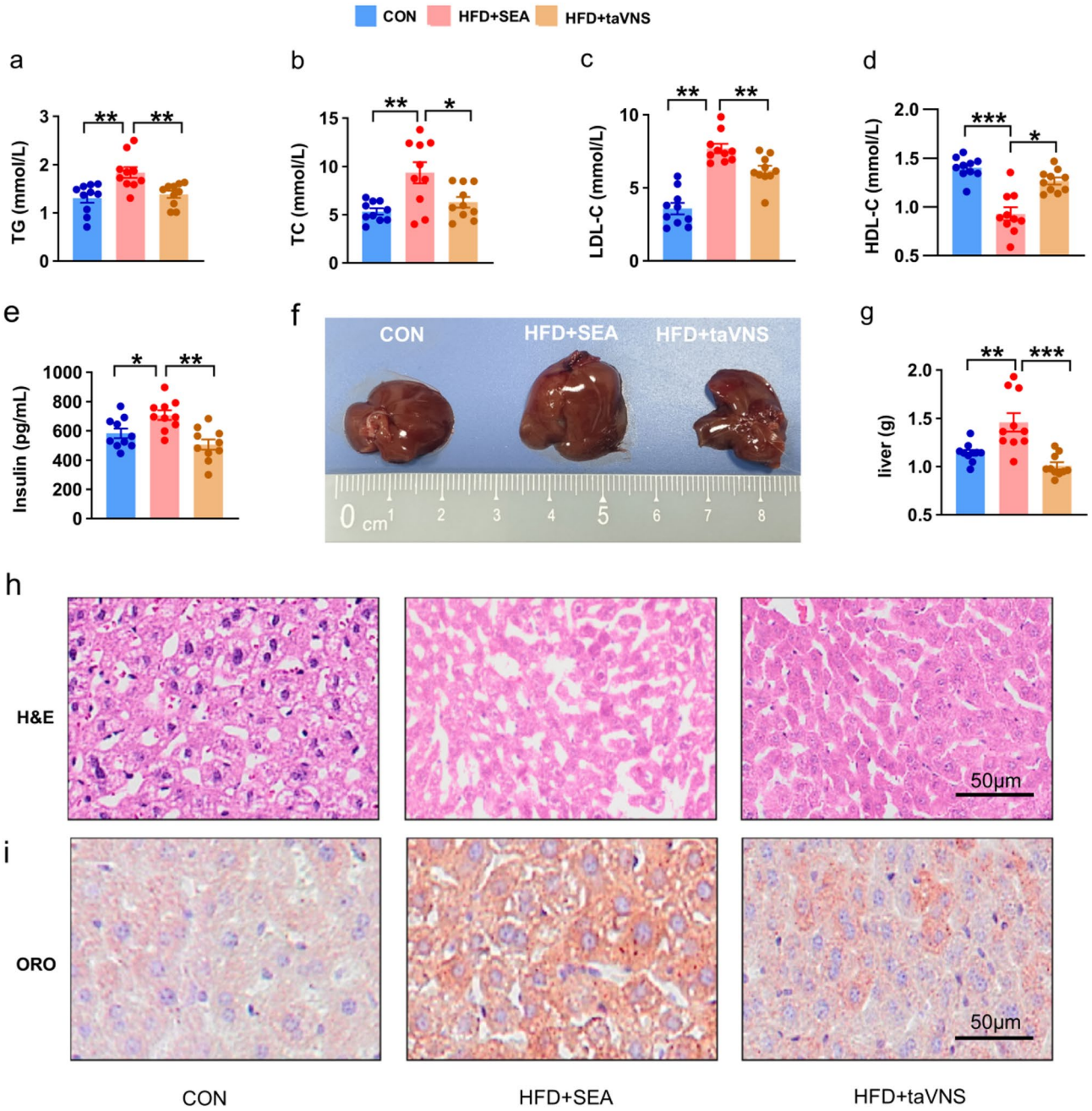

Fig. 2. taVNS significantly improving blood lipid abnormalities. (**a**–**d**) TG (Triglycerides), TC (Total Cholesterol), LDL-C (Low-Density Lipoprotein Cholesterol), and HDL-C (High-Density Lipoprotein Cholesterol) levels in each group. (**e**) Insulin levels in mice. (**f**–**g**) Liver wet weight and change. (**h**–**i**) HE (Hematoxylin and Eosin) staining and Oil Red O staining of mice liver. Statistical significance was denoted as$^{*}P<0.05$, $^{**}P<0.01$,$^{***}P<0.001$.

TaVNS ameliorates lipid deposition and injury in mice liver

Non-alcoholic fatty liver disease is characterized by excessive fat accumulation in the liver, potentially giving rise to an array of health concerns, such as insulin resistance, dyslipidemia, and hypertension[15]. The Oil Red O and HE staining were conducted to assess the pathological condition of the liver. According to the HE staining results (Fig. 2h), the liver tissue of the HFD + SEA group mice presented an unclear liver lobule structure, severe congestion of the central veins, disordered arrangement of hepatic cords, infiltration of local inflammatory cells, swelling and deformation of some liver cells, and cytoplasmic fat vacuoles of varying sizes. The results of the Oil Red O staining revealed that the HFD + SEA mice exhibited circular granular lipid droplets and diffuse lipid droplets of varying sizes within the cytoplasm of the liver tissue. The intercellular boundaries were either blurred or ruptured, indicating severe lipid accumulation. Conversely, the liver of the HFD + taVNS group mice showed significant alleviation in lipid deposition, with only a small number of small red diffuse lipid droplets observed

(Fig. 2i). These pathological changes were also mitigated by taVNS intervention. To sum up, it can be found that the taVNS intervention ameliorated pathological changes in HFD mice.

TaVNS suppressed the appetite of HFD mice through an orexin dependent pathway

The aforementioned results suggested that the appetite of HFD mice decreased due to taVNS, thus initiating the research on its underlying mechanism. Orexins, also referred to as hypothalamic secretins, are a class of neuropeptides that play crucial physiological roles in feeding, sleep[16], reward, and energy balance[17]. Furthermore, we measured the levels of orexin A in the serum and observed a decrease in the HFD + taVNS group compared to the HFD + SEA group (Fig. 3a, $F_{(2, 27)} = 12.28$, $p = 0.0002$). It was posited that taVNS might influence the appetite via an orexin dependent pathway. To validate this hypothesis, almorexant (Alm), an orexin receptor (OXR) antagonist, was administered orally at a dose of 1 mg/kg (Fig. 3b). After 7 days of administration, the HFD + taVNS + Alm group exhibited a significant reduction in body weight, daily food and blood glucose intake compared to the HFD + SEA group, an effect comparable to that of taVNS (Fig. 3c, $F_{(3, 36)} = 11.77$, $p < 0.0001$; Fig. 3d, $F_{(3, 36)} = 13.54$, $p < 0.0001$; Fig. 3e, $F_{(3, 20)} = 12.23$, $p < 0.0001$; Fig. 3f, $F_{(3, 20)} = 61.32$, $p < 0.0001$; Fig. 3g,

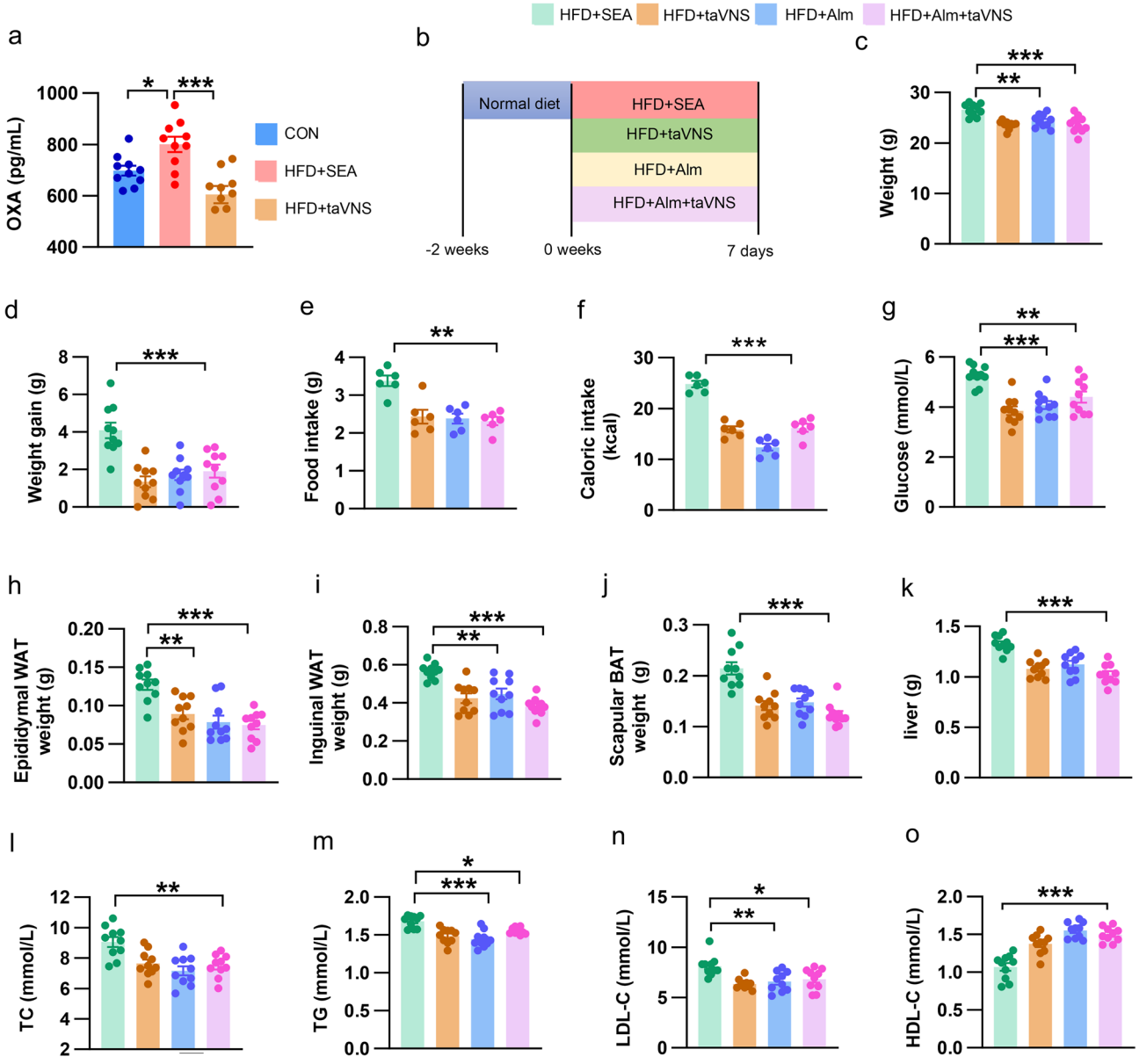

Fig. 3. taVNS reduced food intake by suppressing OXA pathway. (**a**) OXA levels of in plasma of CON, HFD + SEA, HFD + taVNS mice. (**b**) Schematic of the experimental procedure. (**c**, **d**) Body weight and weight gain of CON, HFD + taVNS, HFD + Alm, HFD + taVNS + Alm mice. Almorexant (Alm), OXR antagonist. (**e**–**f** Food and calorie intake of mice after 7 days of oral administration of OXR antagonist. (**g**) FBG levels in mice. (**h**–**j**) Fat pad wet weight in the epididymis, groin, and scapula regions. (**k**) Liver wet weight in mice. (**l**–**o**) TC, TG, LDL-C, and HDL-C levels in mice. Statistical significance was denoted as $^{*}P < 0.05$, $^{**}P < 0.01$, $^{***}P < 0.001$.

$F_{(3, 36)} = 13.25$, $p < 0.0001$). Moreover, the benefits of taVNS on HFD mice could not be further facilitated by almorexant, as evidenced by the dataset on fat weight, fat organ index(Fig. 3h, $F_{(3, 36)} = 11.77$, $p < 0.0001$; Fig. 3i, $F_{(3, 36)} = 14.33$, $p < 0.0001$; Fig. 3j, $F_{(3, 36)} = 18.54$, $p < 0.0001$; Fig. 3k, $F_{(3, 36)} = 19.54$, $p < 0.0001$), TC, TG, LDL, HDL levels (Fig. 3l, $F_{(3, 36)} = 8.774$, $p = 0.0002$; Fig. 3m, $F_{(3, 36)} = 14.29$, $p < 0.0001$; Fig. 3n, $F_{(3, 36)} = 7.438$, $p = 0.0005$; Fig. 3o, $F_{(3, 36)} = 28.68$, $p < 0.0001$). Thus, these results suggested taVNS may exert its benefits on HFD mice through an orexin related pathway.

taVNS suppressed the appetite of HFD mice by inhibiting orexin secretion in LH neurons

Substantial evidence supports the critical role of LH in the control of feeding behavior[18,19]. Early studies with electrolytic lesions and electrical stimulations identified the LH as a "feeding center" in the brain[20,21]. In order to further verify whether orexin derived from LH mediates taVNS' function, LH was inhibited or activated by injecting the viruses expressing the chemogenetic tool hM4D (Gi) /hM3D (Gq) respectively (Fig. 4a–c). Four weeks after viral injection, HFD was administered along with DREADDs (0.5 mg/kg, intraperitoneally, daily). Benefits of taVNS on HFD mice were attenuated by LH activation and could not be enhanced by LH inhibition (Fig. 4d, $F_{(3, 36)} = 77.75$, $p < 0.0001$; Fig. 4e, $F_{(3, 36)} = 154.7$, $p < 0.0001$; Fig. 4f, $F_{(3, 20)} = 32.63$, $p < 0.0001$; Fig. 4g, $F_{(3, 20)} = 32.63$, $p < 0.0001$; Fig. 4h, $F_{(3, 36)} = 32.58$, $p < 0.0001$; Fig. 4i, $F_{(3, 36)} = 34$, $p < 0.0001$; Fig. 4j, $F_{(3, 36)} = 12.47$, $p < 0.0001$; Fig. 4k, $F_{(3, 36)} = 48.31$, $p < 0.0001$; Fig. 4l, $F_{(3, 36)} = 39.97$, $p < 0.0001$; Fig. 4m, $F_{(3, 36)} = 11.63$, $p < 0.0001$;

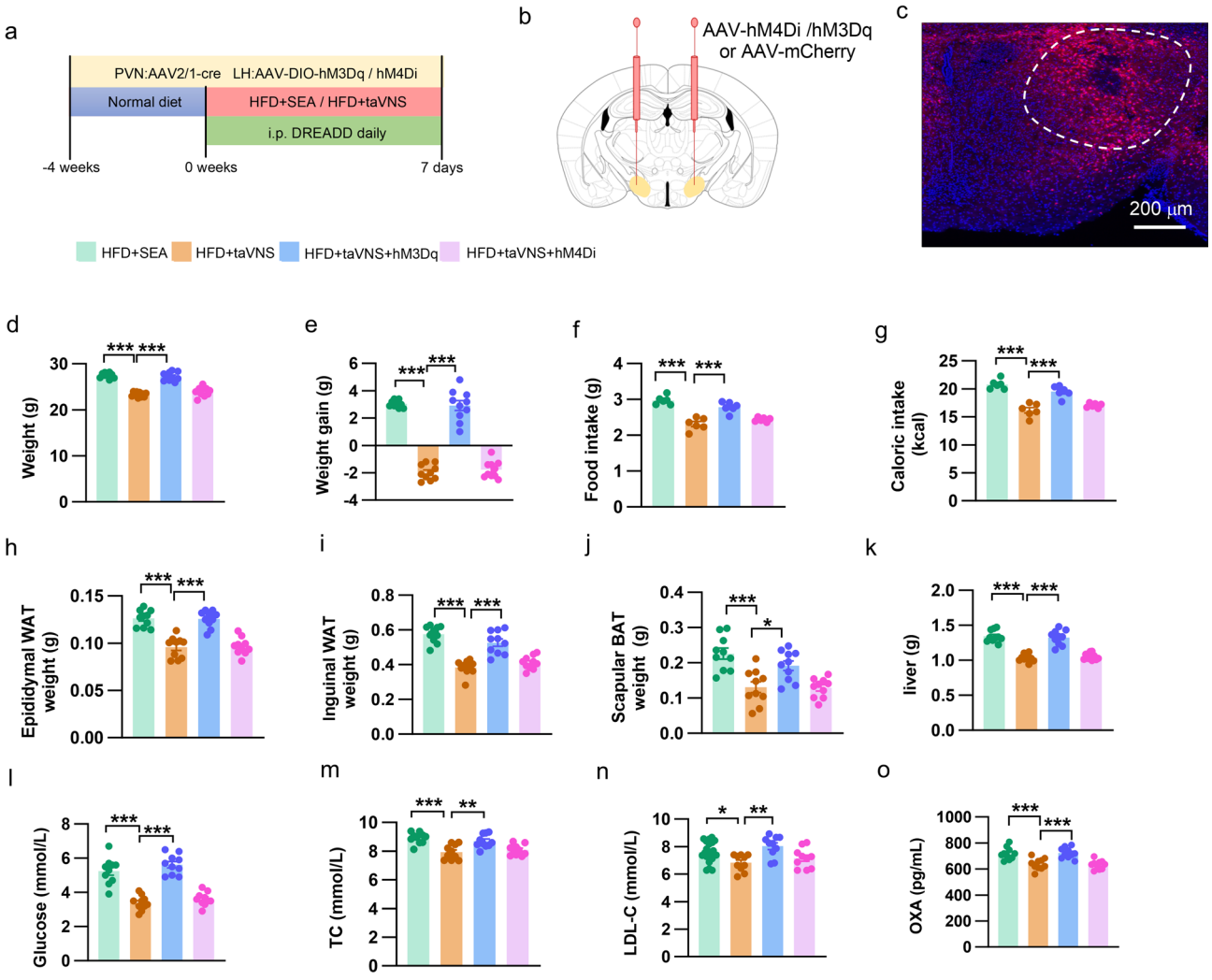

Fig. 4. Chemical genetic activating LH neurons blocked the effects of taVNS on reducing feeding, body weight, or improving blood lipid abnormalities. (**a**) Schematic of the experimental procedure. (**b**) Schematic diagram of injecting chemogenetic virus into the LH brain region of mice. (**c**) Representative image of virus expression in the LH. (**d**–**e**) Weight and weight gain in mice after chemical genetic regulation of LH. (**f**–**g**) Chemical genetic regulation of food and calorie intake in mice. (**h**–**j**) Fat pad wet weight in the epididymis, groin, and scapula regions. (**k**) Liver wet weight of different groups mice. (**l**) FBG levels of different groups mice. (**m**–**n**) Blood lipid levels of different groups mice. (**o**) The concentration of OXA in plasma of different groups mice. $n = 10$ in each group. Statistical significance was denoted as $^{*}P < 0.05$, $^{**}P < 0.01$, $^{***}P < 0.001$.

Fig. 4n, $F_{(3, 36)} = 5.332$, $p = 0.0031$; Fig. 4o, $F_{(3, 36)} = 14.58$, $p < 0.0001$). These results also suggested that suppression of LH neurons was essential for taVNS' benefits.

taVNS decreased orexin level by activating PVN-LH projection

To verify the underlying brain areas mediating taVNS suppressing LH activity, c-FOS staining was utilized to illustrate the activated neurons[22] in the whole brain. Results showed that there was a notable increase in c-FOS positive neurons in the PVN of the HFD mice following taVNS (Fig. 5a, $F_{(2, 6)} = 48$, $p = 0.0002$), leading to the assumption of a neuronal connection between the ear canal (the site of taVNS) and PVN. To test this hypothesis, Pseudorabies virus expressing EGFP (PRV-CAG-EGFP), as a neuroretrograde tracer, was injected into the ear canal to reveal the connectivity patterns of neural circuits. Through this method, PRV markers in the PVN

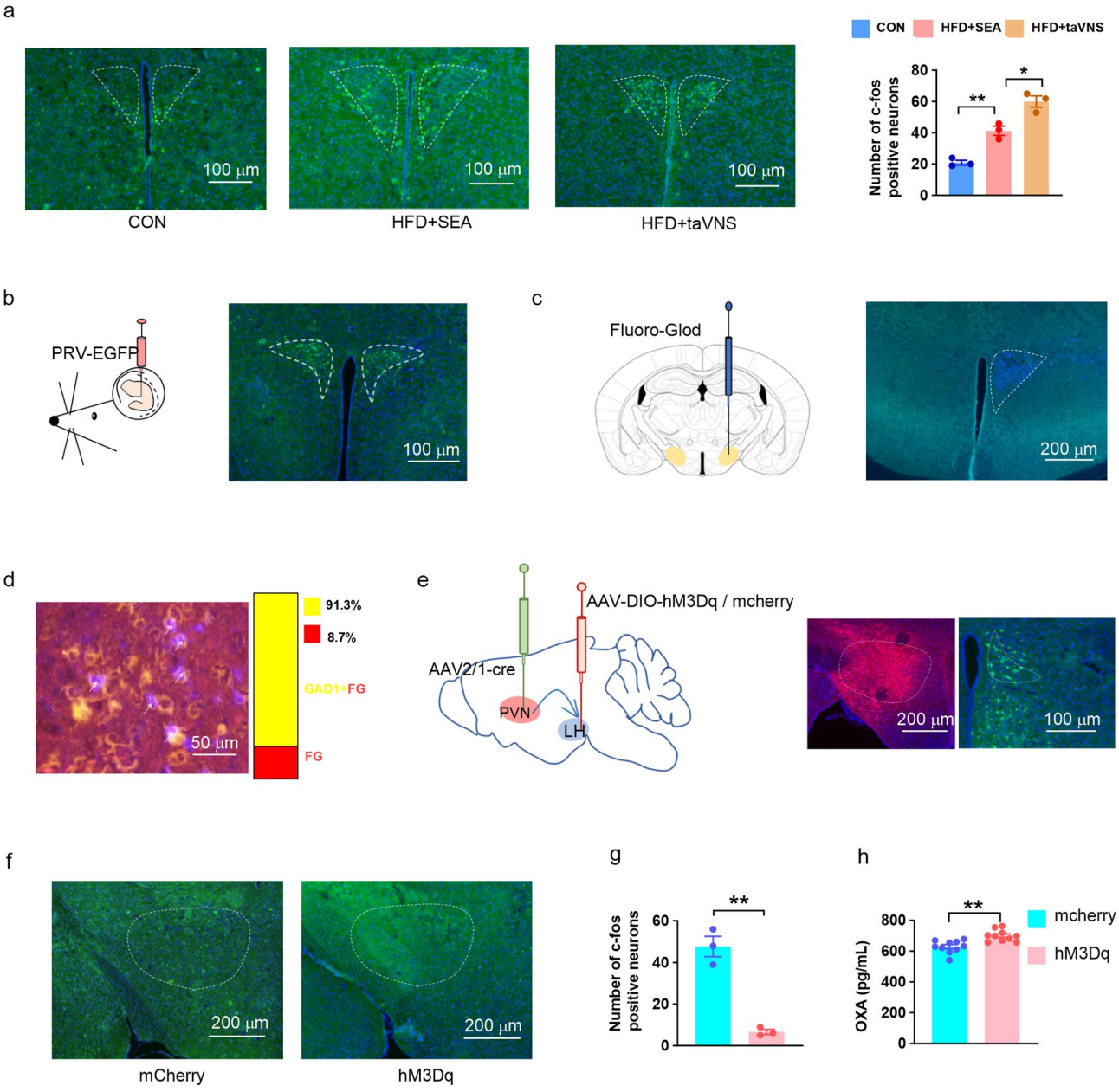

Fig. 5. taVNS suppressed LH activity by activating the LH projecting PVN GABAergic neurons. (**a**) Immunofluorescence staining revealed c-FOS positive neurons in the PVN of different groups of mice. (**b**) Image illustrating of PRV-EGFP injection in the cymba concha and EGFP positive cells in the PVN. (**c**) Image illustrating of FG injection in the LH and LH positive cells in the PVN. (**d**) Ratio of GAD1 and FG double-positive cells and FG single-positive cells in the PVN. (**e**) Schematic and representative image of AAV2/1-Cre injected in the PVN and AAV-DIO-hM3Dq injected in the LH. (**f**–**g**) Number of c-FOS positive cells after activating PVN-LH projection. (**h**) OXA levels in the plasma after activating PVN-LH projection. $n = 3$ in each group. Statistical significance was denoted as $^{*}P < 0.05$, $^{**}P < 0.01$.

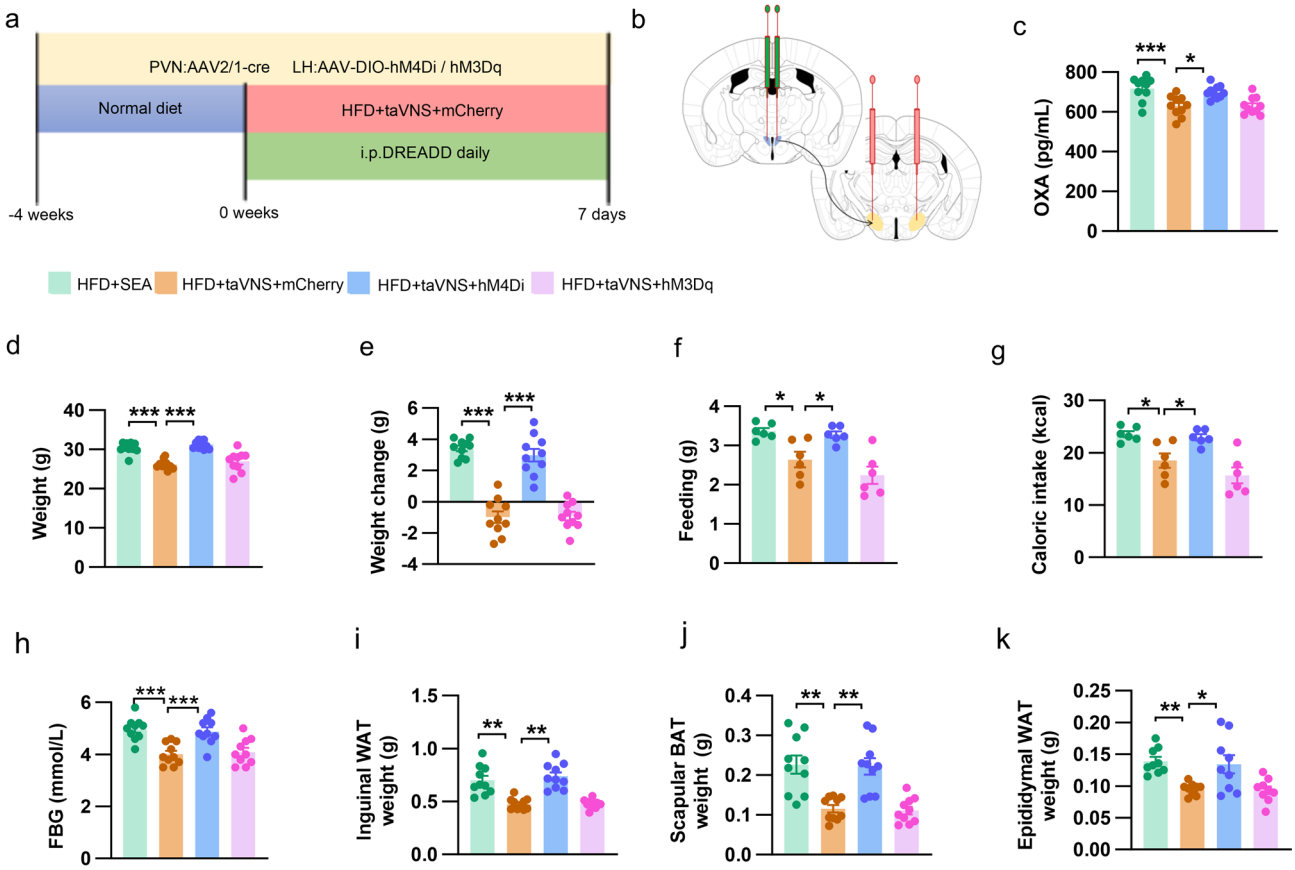

Fig. 6. taVNS suppressed appetite of HFD mice by activating the LH projecting PVN GABAergic neurons. (**a**) Schematic of the experimental procedure. (**b**) Schematic of AAV2/1-Cre injected in the PVN and AAV-DIO-hM3Dq injected in the LH. (**c**) OXA levels in the plasma from HFD mice after inhibiting or activating PVN-LH projection. (**d**, **e**) Body weight and weight gain after inhibiting or activating PVN-LH projection. (**f**–**g**) Food and calorie intake in mice after inhibiting or activating PVN-LH projection. (h) FBG levels in mice after inhibiting or activating PVN-LH projection. (**i**–**k**) Fat pad wet weight in the epididymis, groin, and scapula regions of mice after inhibiting or activating PVN-LH projection. $n = 10$ in each group. $^{*}P < 0.05$, $^{**}P < 0.01$,$^{***}P < 0.001$.

brain region became explicit, suggesting the presence of neural projections between the cymba conchae nail and PVN (Fig. 5b). Then, the retrograde dye FG was injected into the LH region for investigating the neural connection between PVN and LH. Some FG positive cells were detected in the PVN, suggesting that LH received direct neuronal projection from PVN (Fig. 5c). Further immunohistochemical analysis showed that most of the retrograde labeled neurons co-localized with glutamate decarboxylase 1 (GAD1) immunostaining (Fig. 5d). GAD1 serves as a key enzyme responsible for converting glutamate into GABA, which plays a central role in neuroinhibitory transmission[23]. Therefore, these results indicated PVN projected to LH through inhibitory GABA neurons. In order to regulate this projection, this research injected anterograde AAV2/1-cre into PVN and Cre dependent hM3Dq into LH to activate this neural circuit (Fig. 5e). And there was a significant decrease in c-FOS positive cells in the LH brain region after PVN activation (Fig. 5f, and g, $t = 8.110$, $df = 4$), whereas the OXA levels in mice were also significantly reduced (Fig. 5h, $t = 4.028$, $df = 18$). These results indicated taVNS activated PVN^{GABA} -LH projection.

taVNS decreased food intake and weight gain by activating PVN^{GABA}-LH projection

To further validate the role of PVN^{GABA} -LH projection in the taVNS' suppression of food intake and weight gain, this projection was regulated by chemogenetic methods in HFD mice (Fig. 6a,b). By injecting AAV2/1-Cre virus into both sides of the PVN brain region, Cre dependent hM3Dq /hM4Di expression was induced in the LH of mice. Four weeks later, DREADD was injected to activate or inhibit this PVN -LH this projection. It can be observed that chemogenetic activation of the PVN-LH projection decreased the OXA level in the plasma. Conversely, inhibiting the PVN-LH projection elevated OXA levels (Fig. 6c, $F_{(3, 36)} = 9.459$, $p < 0.0001$). Furthermore, benefits of taVNS on HFD mice were blocked by activating PVN-LH, whereas further facilitation was not achieved by inhibiting PVN-LH projection (Fig. 6d, $F_{(3, 36)} = 23.42$, $p < 0.0001$; Fig. 6e, $F_{(3, 36)} = 56.55$, $p < 0.0001$; Fig. 6f, $F_{(3, 20)} = 11.36$, $p = 0.0001$; Fig. 6g, $F_{(3, 20)} = 11.36$, $p = 0.0001$; Fig. 6h, $F_{(3, 36)} = 12.15$, $p < 0.0001$; Fig. 6i, $F_{(3, 36)} = 21.21$, $p < 0.0001$; Fig. 6j, $F_{(3, 36)} = 14.35$, $p < 0.0001$; Fig. 6k, $F_{(3, 36)} = 7.984$, $p = 0.0004$). These

findings confirmed the crucial role of the PVN-LH projection in mediating taVNS' suppression of food intake and weight gain in the HFD mice.

Discussion

In this study, we used short-term HFD mice to investigate the effects of taVNS on body weight gain and food intake. In further research, we found that taVNS activates PVN GABAergic neurons to suppress LH activity and decrease orexin levels in the plasma, thus inhibiting food intake and body weight gain in the HFD mice. Satiety signals are produced by mechanoreceptors and chemoreceptors of the gastrointestinal tract and transmitted via the vagus nerve to the LH, thereby generating appetite—suppressing signals[24]. The LH is a critical brain region involved in regulating dietary behaviors, often referred to as the hunger center. Notably, LH damage has been shown to inhibit food intake, whereas electrical stimulation of the LH can enhance food consumption. This suggests that the LH plays a vital role in maintaining energy homeostasis throughout the eating process[25,26]. Our results indicated that PVN sent GABAergic projection to the LH, thus taVNS suppresses food intake by activating PVN. Furthermore, PVN was also activated by some mental stress accompanied with decreased appetite[27], which is consistent with our findings. However, the difference of PVN activation by mental stress or taVNS still needs further research.

Orexin is a neuropeptide secreted by the LH that plays a crucial role in regulating feeding behavior, sleep-wake rhythms, reward and addiction, and energy balance. Drugs targeting orexin receptors have certain potential in weight loss by regulating appetite and energy expenditure[28]. Activation of orexin receptors can enhance spontaneous physical activity and energy expenditure without impacting food intake, thereby improving fat distribution in a high-calorie dietary environment. Conversely, orexin receptor antagonists can reduce appetite and food intake. Consequently, they are primarily utilized in the treatment of obesity and other disorders associated with overeating. In this research, the involvement of orexins in taVNS mediated weight loss was found, supporting the vital role of orexin in appetite regulation.

The global prevalence of obesity and related diseases continues to rise, leading to a significant increase in prevention and treatment costs[29]. Due to the lack safety weight loss drugs, the importance of achieving weight loss through non pharmacological and non-surgical means is emphasized. Previous studies have shown that VNS can regulate food intake and body weight in rats and mice in the short term, leading to a reduction in weight gain[30,31]. These studies provide preliminary evidence for VNS as a potential treatment for obesity. However, traditional VNS needs a surgical operation to implant the electrode and is associated with risk of infection. As the presence of afferent projections of the vagus nerve in the cymba conchae and external ear canals of mammals[32], taVNS has been developed, offering a non-invasive stimulation way. As a newly developed method, taVNS has shown benefits for various diseases, including epilepsy[33], chronic tinnitus[34], depression[35], functional dyspepsia[36] and insomnia[37]. Improvements and innovations in stimulating equipment have also enhanced both the safety and effectiveness of taVNS.

Data availability

The data underlying this article will be shared upon reasonable request to the corresponding author.

Received: 16 December 2024; Accepted: 9 May 2025
Published online: 02 June 2025

References

1. Hariri, N. & Thibault, L. High-fat diet-induced obesity in animal models. *Nutr. Res. Rev.* **23**, 270–299. https://doi.org/10.1017/S0954422410000168 (2010).
2. Hill, J. O. & Peters, J. C. Environmental contributions to the obesity epidemic. *Science* **280**, 1371–1374. https://doi.org/10.1126/science.280.5368.1371 (1998).
3. Wheless, J. W., Gienapp, A. J. & Ryvlin, P. Vagus nerve stimulation (VNS) therapy update. *Epilepsy Behav.* **88S**, 2–10. https://doi.org/10.1016/j.yebeh.2018.06.032 (2018).
4. Connolly, S. D., Suarez, L. & Sylvester, C. Assessment and treatment of anxiety disorders in children and adolescents. *Curr. Psychiatry Rep.* **13**, 99–110. https://doi.org/10.1007/s11920-010-0173-z (2011).
5. Neren, D. et al. Vagus nerve stimulation and other neuromodulation methods for treatment of traumatic brain injury. *Neurocrit. Care* **24**, 308–319. https://doi.org/10.1007/s12028-015-0203-0 (2016).
6. Farrand, A. Q. et al. Vagus nerve stimulation improves locomotion and neuronal populations in a model of Parkinson's disease. *Brain Stimul.* **10**, 1045–1054. https://doi.org/10.1016/j.brs.2017.08.008 (2017).
7. Peuker, E. T. & Filler, T. J. The nerve supply of the human auricle. *Clin. Anat.* **15**, 35–37. https://doi.org/10.1002/ca.1089 (2002).
8. Wang, Y. et al. Transcutaneous auricular vagus nerve stimulation: From concept to application. *Neurosci. Bull.* **37**, 853–862. https://doi.org/10.1007/s12264-020-00619-y (2021).
9. Gil, K., Bugajski, A. & Thor, P. Electrical vagus nerve stimulation decreases food consumption and weight gain in rats fed a high-fat diet. *J. Physiol. Pharmacol.* **62**, 637–646 (2011).
10. Laskiewicz, J. et al. Effects of vagal neuromodulation and vagotomy on control of food intake and body weight in rats. *J. Physiol. Pharmacol.* **54**, 603–610 (2003).
11. Vazquez-Oliver, A. et al. Auricular transcutaneous vagus nerve stimulation improves memory persistence in Naive mice and in an intellectual disability mouse model. *Brain Stimul.* **13**, 494–498. https://doi.org/10.1016/j.brs.2019.12.024 (2020).
12. Hong, G. S. et al. Non-invasive transcutaneous auricular vagus nerve stimulation prevents postoperative ileus and endotoxemia in mice. *Neurogastroenterol. Motil.* **31**, e13501. https://doi.org/10.1111/nmo.13501 (2019).
13. Rosen, E. D. & Spiegelman, B. M. What we talk about when we talk about fat. *Cell* **156**, 20–44. https://doi.org/10.1016/j.cell.2013.12.012 (2014).
14. Vishvanath, L. & Gupta, R. K. Contribution of adipogenesis to healthy adipose tissue expansion in obesity. *J. Clin. Invest.* **129**, 4022–4031. https://doi.org/10.1172/JCI129191 (2019).
15. Lee, E. S. et al. Curcumin analog CUR5-8 ameliorates nonalcoholic fatty liver disease in mice with high-fat diet-induced obesity. *Metabolism* **103**, 154015. https://doi.org/10.1016/j.metabol.2019.154015 (2020).

16. Willie, J. T., Chemelli, R. M., Sinton, C. M. & Yanagisawa, M. To eat or to sleep? Orexin in the regulation of feeding and wakefulness. *Annu. Rev. Neurosci.* **24**, 429–458. https://doi.org/10.1146/annurev.neuro.24.1.429 (2001).
17. Mavanji, V., Pomonis, B. & Kotz, C. M. Orexin, serotonin, and energy balance. *WIREs Mech. Dis.* **14**, e1536. https://doi.org/10.1002/wsbm.1536 (2022).
18. Hoebel, B. G. & Teitelbaum, P. Hypothalamic control of feeding and self-stimulation. *Science* **135**, 375–377. https://doi.org/10.1126/science.135.3501.375 (1962).
19. Stuber, G. D. & Wise, R. A. Lateral hypothalamic circuits for feeding and reward. *Nat. Neurosci.* **19**, 198–205. https://doi.org/10.1038/nn.4220 (2016).
20. Nutrition Classics. The anatomical record, volume 78: Hypothalamic lesions and adiposity in the rat. *Nutr. Rev.* **41**, 124–127 (1983). https://doi.org/10.1111/j.1753-4887.1983.tb07169.x
21. Anand, B. K. & Brobeck, J. R. Localization of a feeding center in the hypothalamus of the rat. *Proc. Soc. Exp. Biol. Med.* **77**, 323–324. https://doi.org/10.3181/00379727-77-18766 (1951).
22. Cruz-Mendoza, F., Jauregui-Huerta, F., Aguilar-Delgadillo, A., Garcia-Estrada, J. & Luquin, S. Immediate early gene c-fos in the brain: Focus on glial cells. *Brain Sci.* **12**. https://doi.org/10.3390/brainsci12060687 (2022).
23. Chen, Y., Dong, E. & Grayson, D. R. Analysis of the GAD1 promoter: Trans-acting factors and DNA methylation converge on the 5' untranslated region. *Neuropharmacology* **60**, 1075–1087. https://doi.org/10.1016/j.neuropharm.2010.09.017 (2011).
24. Gong, Y. et al. Ghrelin fibers from lateral hypothalamus project to nucleus tractus solitaries and are involved in gastric motility regulation in cisplatin-treated rats. *Brain Res.* **1659**, 29–40. https://doi.org/10.1016/j.brainres.2017.01.004 (2017).
25. Sharpe, M. J. The cognitive (lateral) hypothalamus. *Trends Cogn. Sci.* **28**, 18–29. https://doi.org/10.1016/j.tics.2023.08.019 (2024).
26. Yonemochi, N., Ardianto, C., Ueda, D., Kamei, J. & Ikeda, H. GABAergic function in the lateral hypothalamus regulates feeding behavior: Possible mediation via orexin. *Neuropsychopharmacol. Rep.* **39**, 289–296. https://doi.org/10.1002/npr2.12080 (2019).
27. Daviu, N. et al. Paraventricular nucleus CRH neurons encode stress controllability and regulate defensive behavior selection. *Nat. Neurosci.* **23**, 398–410. https://doi.org/10.1038/s41593-020-0591-0 (2020).
28. Perez-Leighton, C. E., Butterick-Peterson, T. A., Billington, C. J. & Kotz, C. M. Role of orexin receptors in obesity: From cellular to behavioral evidence. *Int. J. Obes. (Lond)* **37**, 167–174. https://doi.org/10.1038/ijo.2012.30 (2013).
29. Lin, X. & Li, H. Obesity epidemiology, pathophysiology, and therapeutics. *Front. Endocrinol. (Lausanne)* **12**, 706978. https://doi.org/10.3389/fendo.2021.706978 (2021).
30. Pelot, N. A. & Grill, W. M. Effects of vagal neuromodulation on feeding behavior. *Brain Res.* **1693**, 180–187. https://doi.org/10.1016/j.brainres.2018.02.003 (2018).
31. Val-Laillet, D., Biraben, A., Randuineau, G. & Malbert, C. H. Chronic vagus nerve stimulation decreased weight gain, food consumption and sweet craving in adult obese minipigs. *Appetite* **55**, 245–252. https://doi.org/10.1016/j.appet.2010.06.008 (2010).
32. He, W. et al. Auricular acupuncture and vagal regulation. *Evid. Based Complement. Alternat Med.* **2012**, 786839. https://doi.org/10.1155/2012/786839 (2012).
33. Zhang, Q. et al. Transcutaneous auricular vagus nerve stimulation for epilepsy. *Seizure* **119**, 84–91. https://doi.org/10.1016/j.seizure.2024.05.005 (2024).
34. Ylikoski, J. et al. Stress and tinnitus; transcutaneous auricular vagal nerve stimulation attenuates tinnitus-triggered stress reaction. *Front. Psychol.* **11**, 570196. https://doi.org/10.3389/fpsyg.2020.570196 (2020).
35. Wang, J. Y. et al. Mechanisms underlying antidepressant effect of transcutaneous auricular vagus nerve stimulation on CUMS model rats based on hippocampal alpha7nAchR/NF-kappaB signal pathway. *J. Neuroinflamm.* **18**, 291. https://doi.org/10.1186/s12974-021-02341-6 (2021).
36. Zhu, Y. et al. Transcutaneous auricular vagal nerve stimulation improves functional dyspepsia by enhancing vagal efferent activity. *Am. J. Physiol. Gastrointest. Liver Physiol.* **320**, G700–G711. https://doi.org/10.1152/ajpgi.00426.2020 (2021).
37. Zhao, B. et al. Altered functional connectivity of the thalamus in patients with insomnia disorder after transcutaneous auricular vagus nerve stimulation therapy. *Front. Neurol.* **14**, 1164869. https://doi.org/10.3389/fneur.2023.1164869 (2023).

Acknowledgements

This research was supported by Key Laboratory of Acupuncture & Medicine of Shaanxi Province, Shaanxi University of Chinese Medicine (No. KF202319), Research Institution, Xijing Hospital (No. LHJJ2023-YX08), National Natural Science Foundation of China (No. 82471537).

Author contributions

Yingying Zhang: Writing—original draft, Investigation. Dake Song: Investigation. Ruixia Liu: Investigation. Hengxin Gong: Data curation. Chuan Wang: Supervision, Methodology. Ming-gao Zhao: Writing—review & editing, Supervision. Kun Zhang: Writing—review & editing, Supervision, Methodology, Conceptualization.

Declarations

Competing interests

The authors declare no competing interests.

Additional information

Supplementary Information The online version contains supplementary material available at https://doi.org/10.1038/s41598-025-01964-6.

Correspondence and requests for materials should be addressed to M.-g.Z. or K.Z.